

Incorporation of RGS losses into BMAD, following implementation of Touschek losses

Note: This document has been edited to “Lab Book” quality.

1 Introduction

Residual Gas Scattering (RGS) occurs when beam particles collide with residual gas molecules. The energy or angle of the beam particle is changed during the collision. The change in energy or angle can result in the particle colliding with the beam chamber downstream of the scattering event. When the particle is lost to the beam chamber, Bremsstrahlung is produced. This Bremsstrahlung can pose a radiation hazard. Because of this radiation hazard, the generation and loss of RGS particles must be examined in detail.

The simulation of RGS losses is similar to that of Touschek losses. Both are single-event scattering processes that change the phase-space coordinate of the colliding particles, resulting in particle loss downstream of the scattering event. Both processes can be succinctly described by distribution functions that give the rate at which particles with perturbed phase-space coordinates are generated.

Touschek loss simulations have already been implemented in BMAD. Since the simulation of RGS losses and Touschek losses are similar, the RGS loss simulations will be based upon the already developed Touschek loss simulations.

One difference between RGS and Touschek losses are the scattering cross-sections. The other difference is that Touschek losses occur only in the horizontal plane, while RGS deflects particles into both the vertical and horizontal plane.

Dealing with the first difference is simple. Closed formulas for the RGS scattering cross-sections are contained in The Handbook. These formulas can be integrated over Gaussian beam distributions to obtain formulas for the rate at which scattered particles are generated.

First, the aperture of the accelerator must be determined in both x and y. To improve accuracy, the aperture should be determined for several values of azimuth. For example, at $\phi = 0, \pi/4, \pi/2, 3\pi/4, \dots, 7\pi/4$. Determining the aperture for various values of ϕ will be more computationally intensive than determining it in only the horizontal plane, but since the aperture program is now parallelized with MPI, the additional computational time will not be prohibitive. A parallelized phase_space_aperture program will be written that calculates the aperture in phase space at each element in the accelerator.

Second, since RGS scatters into all azimuthal angles with equal probability, a distribution of particles will be generated for each azimuthal angle in the data file. The distributions will each be reduced by a factor equal to the number of ϕ in the aperture file.

2 Scattering Cross-Sections

Residual Gas Scattering has two uncorrelated cross-sections. These are in Section 3.3.1 of The Handbook. We are interested in “Single Coulomb scattering of spin-1/2 particles” and “Bremsstrahlung on gas nuclei”. Coulomb scattering is described by a differential cross-section as a function of zenith. Bremsstrahlung is described by a differential cross-section as a function of fractional energy loss. The two cross-sections are uncorrelated.

2.1 Angle change due to Coulomb scattering

Equation 3.3.1.2 from The Handbook gives the differential cross-section for Coulomb scattering as,

$$\frac{d\sigma}{d\Omega} \approx 4Z^2 r_e^2 \frac{1}{(\theta^2 + \theta_{th}^2)^2} \left(\frac{m_e c}{\beta p} \right)^2, \quad (1)$$

where $\theta_{th} \approx \alpha Z^{1/3} (m_e c/p)$. Note that $m_e c/\beta p = \gamma/(\gamma^2 - 1)$.

Equation 1 is integrated from the threshold divergence for particle loss, θ_{min} , and π to obtain the total cross section for particle loss. The result is,

$$\sigma_{coul} = 8\pi Z^2 r_e^2 \left(\frac{\gamma}{\gamma^2 - 1} \right)^2 \int_{\theta_{min}}^{\pi} \frac{1}{(\theta^2 + \theta_{th}^2)^2} \sin[\theta] d\theta \quad (2)$$

$$= 8\pi Z^2 r_e^2 \left(\frac{\gamma}{\gamma^2 - 1} \right)^2 \times (F[\pi] - F[\theta_{min}]), \quad (3)$$

where,

$$F[\theta] = -\frac{1}{8\theta_{th}^3} \left(e^{\theta_{th}} (\theta_{th} - 1) (Ei[-i\theta - \theta_{th}] + Ei[i\theta - \theta_{th}]) + e^{-\theta_{th}} (\theta_{th} + 1) (Ei[-i\theta + \theta_{th}] + Ei[i\theta + \theta_{th}]) - \frac{4\theta_{th} \sin[\theta]}{\theta^2 + \theta_{th}^2} \right), \quad (4)$$

where $Ei[z]$ is the exponential integral Ei. Note that the imaginary part of Ei cancels out exactly in this expression, guaranteeing a real result.

2.2 Bremsstrahlung on gas nuclei

Equation 3.3.1.11 from The Handbook gives the differential cross-section for energy change due to Bremsstrahlung on gas nuclei as,

$$\frac{d\sigma}{du} \approx 4\alpha r_e^2 Z(Z+1) \frac{4}{3u} \left(1 - u + \frac{3}{4}u^2 \right) \log \left[\frac{184.15}{Z^{1/3}} \right], \quad (5)$$

where $u = k/E$ is the fractional energy loss. For example, for a 5 GeV particle that loses 10 MeV, $u = \frac{10\text{MeV}}{5\text{GeV}}$.

The integrated cross-section for a particle to lose an energy between u_{min} and 1 is,

$$\sigma_{brem} = 4\alpha r_e^2 Z(Z+1) \frac{4}{3} \left(-\frac{5}{8} + u_{min} - \frac{3}{8}u_{min}^2 - \log[u_{min}] \right) \log \left[\frac{184.15}{Z^{1/3}} \right]. \quad (6)$$

3 Scattering Rate

Since Eqs. 3 and 6 do not depend on the phase-space coordinates of the scattering particles or Twiss parameters, a simple derivation is sufficient for determining the rate at which RGS particles are produced.

An electron traveling at a velocity v is incident on a box of dimensions dx , dy , and $c\Delta t$ containing a density of gas particles ρ . See Fig. 1. The cross-sectional area of each gas particle is σ . The box contains $N_\rho = \rho dx dy c\Delta t$ particles, which

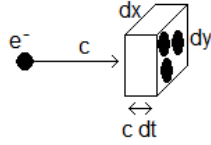


Figure 1: Simple scattering.

cover a combined area $A = \sigma \rho dx dy c\Delta t$. The incident electron has a probability $P = \frac{\sigma \rho dx dy c\Delta t}{dx dy} = \sigma \rho c\Delta t$ of colliding with a gas particle.

A particle traveling through a gas will encounter $\frac{P}{\Delta t} = \sigma \rho c$ collisions per second. If N_p particles are traveling through the gas as speed c , the number of collisions per second will be,

$$\dot{N}_c = N_p n \sigma c. \quad (7)$$

N_p is set to the number of particles per bunch. To find the number of scattered particles generated in an element by each crossing bunch, Eq. 7 is multiplied by l/c , where l is the length of the element.

Because Eqs. 3 and 6 are uncorrelated, they can be treated as separate processes, each producing a separate distribution of scattered particles.

4 Determining Aperture

The accelerator will be divided up into slices about 1 meter long. At each slice, the aperture will be probed at angles spanning 2π of azimuth. The program will find the aperture in θ at $\phi = 0$, then at $\phi = \pi/4$, ..., and finally at $\phi = 7\pi/4$. The aperture in θ will be found using a binary search. The results will be stored in a data file.

For the Bremsstrahlung RGS particles, the existing Touschek aperture file, which contains the negative energy aperture, will be used.

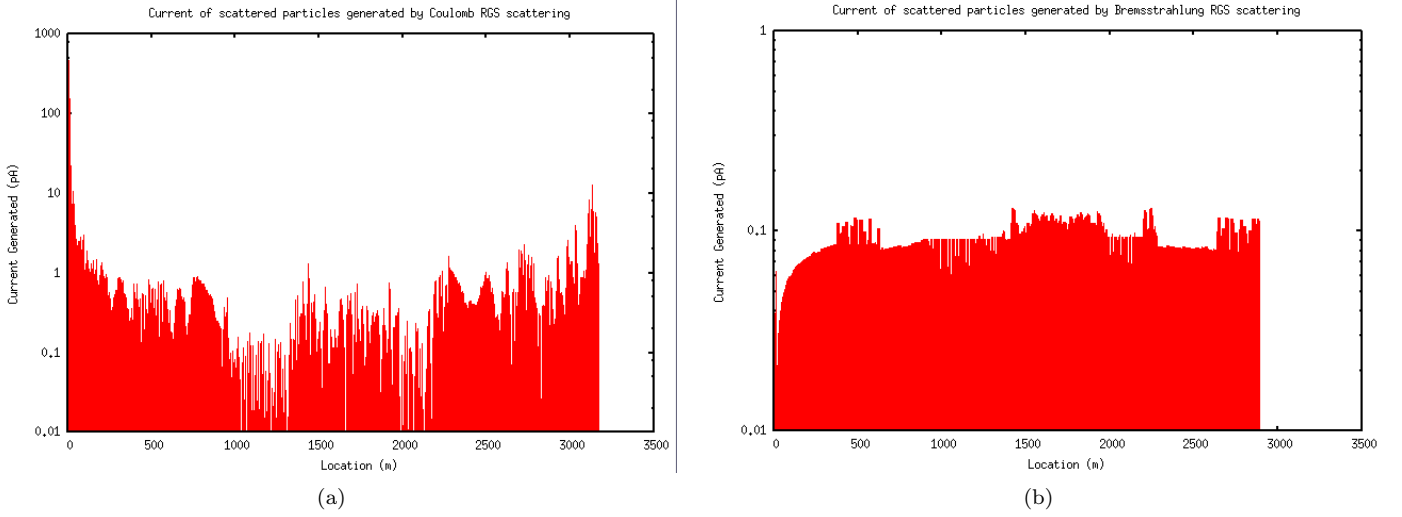


Figure 2: Current of lost particles generated per meter due to RGS scattering.

5 Production and Tracking

Since the dimensions of the beam chamber are much larger than the beam envelop, the initial angle and energy defect of the scattered particles can be ignored. That is, $\delta E/E \ll u$ and $\sqrt{\gamma\epsilon} \ll \theta_m$.

5.1 Coulomb Scattering

At each slice and at each azimuth, as provided by the aperture file, the number of particles scattered outside the aperture will be calculated using $\dot{N}_{coul} [\theta_m, \infty]$. \dot{N}_{coul} will be divided into n test particles. Each test particle will represent a range of scattered particles generated.

The angle change represented by each test particle will be found by algebraically inverting Eq. ?? to obtain $\theta_m [\dot{N}_{brem}]$.

For example, the first test particle will represent particles $[0, \dot{N}_{coul}/n]$ and has an angle $\theta_m [\frac{1}{2}\dot{N}_{coul}/n]$, the second test particle will represent particles $[\dot{N}_{coul}/n, 2\dot{N}_{coul}/n]$ and has an angle $\theta_m [\frac{3}{2}\dot{N}_{coul}/n]$, and so on. The angle changes will be projected into the x-y plane, according to the ϕ being examined.

Finally, the test particles are tracked through the accelerator to where they are lost, and their trajectories are recorded and analyzed.

5.2 Bremsstrahlung on gas nuclei

The production and tracking of the Bremsstrahlung RGS particles is identical to that for Coulomb Scattered RGS particles, except that instead of an angle change, there is an energy defect. There is no need to track for various values of ϕ .

5.3 Data Analysis

The slice-by-slice generation rate and slice-by-slice loss rate will be generated and recorded. The trajectories of the scattered particles will be recorded in a histogram, which can be analyzed to guide collimator placement.

6 Results

Two simulations are produced. One generates and tracks particles produced by Coulomb scattering, the other by Bremsstrahlung. The method for constructing the distributions of scattered particles is the same as that for Touschek particles that is described in “Collimating Touschek particles in an Energy Recovery Linear accelerator,” Proceedings PAC09. The simulation results below are from a CERL 7.4 lattice with wiggler collimators but without Touschek collimators.

Shown in Figs. 2(a) and 2(b) is the current generated per meter due to Coulomb scattering and Bremsstrahlung. The Coulomb scattering rate is very high at the start of the lattice. This is due to the $1/\gamma^2$ dependence in Eq. 3. γ at injection is 20, and peak γ is 10000. Since Bremsstrahlung RGS produces only a momentum defect, it produces no scattered particles after the last bend.

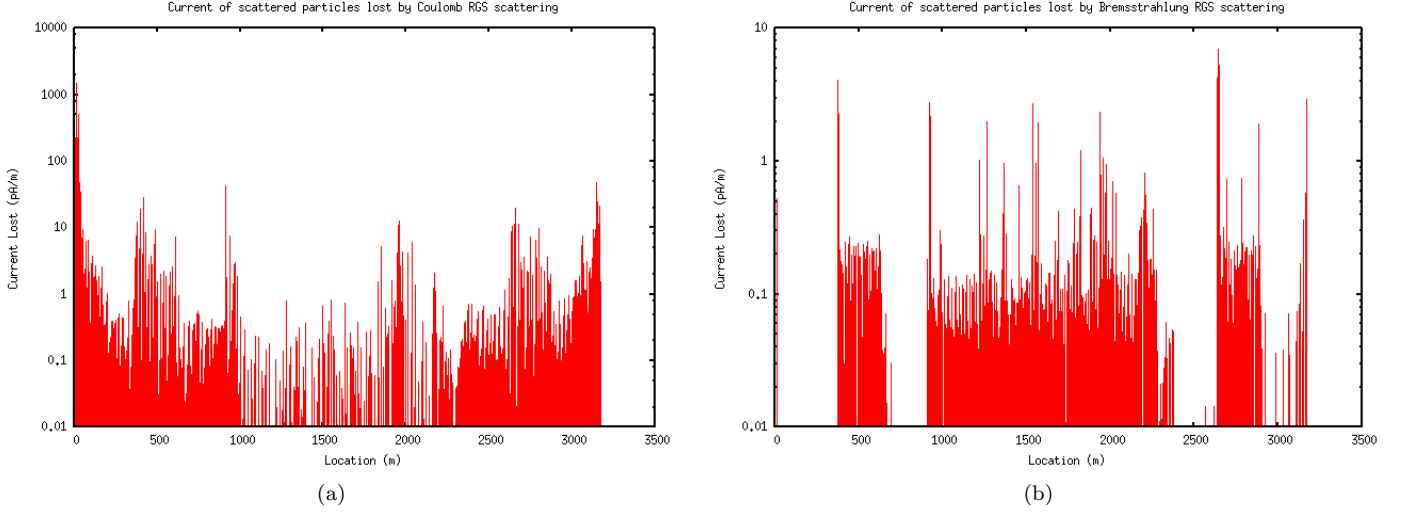


Figure 3: Current of particles lost per meter due to RGS scattering.

Shown in Figs. 3(a) and 3(b) is the current lost per meter due to Coulomb scattering and Bremsstrahlung. Since the Bremsstrahlung process produces only an energy defect, a negligible number of particles are lost in the linacs, where dispersion is zero.

Shown in Fig. 4 is the distribution of Coulomb RGS particles on the first wiggler collimator. The histogram grid is 400 by 400, giving $3.75 \times 10^{-9} \text{ m}^2$ per grid point. Total current is 277.9 pA.

7 Conclusion

Residual Gas Scattering simulations have been implemented in BMAD. The structure of the simulations is very similar to that of the Touschek simulations. The RGS simulations have been run on the CERL 7.4 lattice and reasonable results were given.

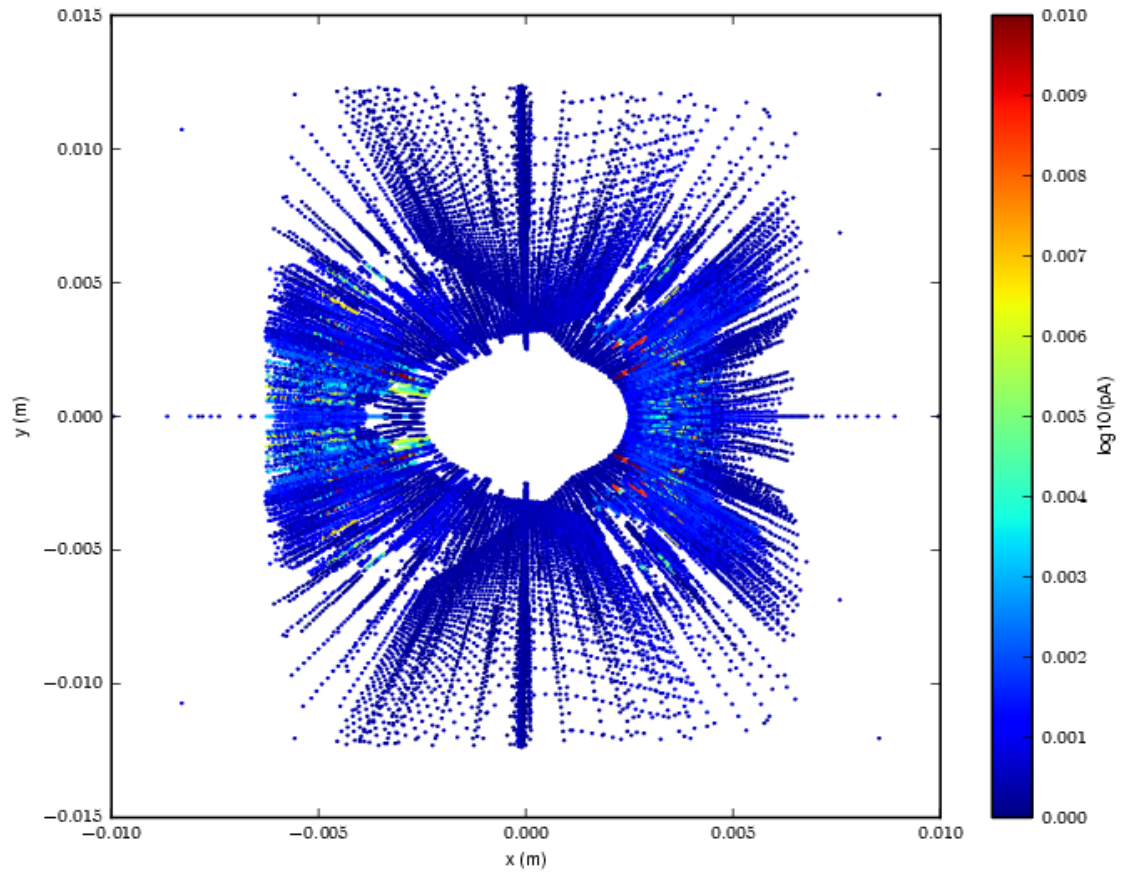


Figure 4: Distribution of Coulomb RGS particles on first wiggler collimator. Total current in 277.9 pA. $3.75 \times 10^{-9} \text{ m}^2$ per grid point.